

Published in final edited form as:

Nat Commun. ; 5: 4460. doi:10.1038/ncomms5460.

Ultra-sensitive optical oxygen sensors for characterisation of nearly anoxic systems

Philipp Lehner, Christoph Staudinger, Sergey M. Borisov*, and Ingo Klimant

Institute of Analytical Chemistry and Food Chemistry Graz University of Technology, NAWI Graz, Stremayrgasse 9, 8010 Graz, Austria

Abstract

Oxygen quantification in trace amounts is essential in many fields of science and technology. Optical oxygen sensors proved invaluable tools for oxygen measurements in a broad concentration range but until now neither optical nor electrochemical oxygen sensors were able to quantify oxygen in the sub-nanomolar concentration range. Herein we present new optical oxygen sensing materials with unmatched sensitivity. They rely on the combination of ultra-long decaying (several hundred milliseconds lifetime) phosphorescent boron- and aluminium-chelates and highly oxygen-permeable and chemically stable perfluorinated polymers. The sensitivity of the new sensors is improved up to 20-fold compared to state-of-the-art analogues. The limits of detection are as low as 5 parts per billion, volume in gas phase under atmospheric pressure or 7 picomolar in solution. The sensors enable completely new applications for monitoring of oxygen in previously inaccessible concentration ranges.

Introduction

Oxygen undoubtedly belongs to the most important analytes on earth. Traditionally, most oxygen sensors were designed for the physiological range. However, numerous applications require monitoring of oxygen at significantly lower concentrations, for example, corrosion protection,¹ surface treatment,² the semiconductor industry³ and biological research. For instance, it was demonstrated that bacteria can show respiration and potentially aerobic growth far below the Pasteur point (about 10 μ M dissolved oxygen).⁴⁻⁶ Recently, sensors that quantify dissolved oxygen (DO) in concentration ranges of 100 nM and below have gained special interest as biologists explore aerobic life in areas very close to anoxic conditions.⁷ Unfortunately, few sensors are capable to resolve at such low concentration,^{8,9} and measurements below 0.5 nM are currently impossible.

Users may view, print, copy, and download text and data-mine the content in such documents, for the purposes of academic research, subject always to the full Conditions of use:http://www.nature.com/authors/editorial_policies/license.html#terms

^[*]sergey.borisov@tugraz.at.

Author Contributions: P.L. designed the measurement set-up, characterized the boron chelates and wrote the paper. C.S. synthesised the aluminium complexes and did the related characterisations and calibrations. S.M.B. synthesized the boron chelates, discovered their interesting properties and performed the initial perfluoroalkylation studies. I.K. supervised the project. All authors contributed substantially to discussion and planning.

Competing financial interests: the authors declare no competing financial interests.

Optical sensors proved to be indispensable tools for oxygen quantification which have mostly replaced the more conventional Clark electrode. Their advantages include minimal invasiveness, simplicity, suitability for miniaturization, versatility of formats (planar optodes, fiber-optic sensors, micro- and nanoparticles, paints, etc.) and suitability for imaging of oxygen distribution on surfaces or in volume. Moreover, optical oxygen sensors are tuneable over a wide range of concentrations. Optical oxygen sensors rely on quenching of a phosphorescent indicator by the analyte. Both the nature of the indicator and the matrix (which acts as a solvent and support for the dye and as a permeation-selective barrier) are of great importance since the sensitivity of an oxygen sensor is roughly proportional to the luminescence decay time of the indicator and to the oxygen permeability of the matrix.¹⁰ State-of-the-art indicators are dominated by phosphorescent complexes with platinum group metals, which possess decay times varying from microseconds to a few milliseconds.¹¹⁻¹⁴ Dyes with significantly longer decay times are extremely rare and are so far limited to fullerenes^{9,15} (which have rather low luminescence brightness at ambient temperatures) and some phosphorescent BF₂ chelates.¹⁶⁻¹⁹ Both classes are not inherently compatible with highly oxygen-permeable matrices (e. g. silicone, Teflon® AF). Hence, the sensors based on these indicators and other matrices (e.g ethyl cellulose, polystyrene)⁹ are not drastically more sensitive than sensors relying on more conventional dyes (e.g. Pd(II) porphyrins) immobilized in highly oxygen-permeable polymers.²⁰

Herein, we present a new type of oxygen-sensing materials that show sensitivities well beyond state-of-the-art trace oxygen sensors. They rely on new blue light-excitable BF₂ and Al(III) chelates featuring ultra-long room temperature phosphorescence. The chelates are modified with perfluoroalkyl chains to ensure compatibility with highly oxygen-permeable and chemically inert perfluorinated polymers. The resulted ultra-sensitive sensors are ideally suitable for characterization of nearly anoxic systems.

Results

Photophysical properties

The new sensing materials rely on novel difluoroboron- and aluminium chelates of 9-hydroxyphenalenone (HPhN, Fig. 1)²¹ and its benzannelated derivative 6-hydroxybenz[de]anthracene-7-on (HBAN, Fig. 1).²² In contrast to the common fluorescent difluoroboron chelates of dipyrromethenes and tetraarylazadipyrromethenes^{23,24} the new difluoroboron-based dyes simultaneously show prompt fluorescence, delayed fluorescence and phosphorescence when embedded in polymers (Fig. 2a, Fig. 2b). Room temperature phosphorescence is an extremely rare phenomenon for compounds with no heavy atoms. It was previously observed for BF₂-chelates of aliphatic β -diketones coupled to polylactic acid^{16,17} or physically entrapped in the same polymer.¹⁹ This work and our results indicate that phosphorescence of aliphatic and aromatic BF₂-chelates of β -diketones appears to be a general phenomenon. As can be seen, the extension of π -conjugation in 9-hydroxyphenalenone derivatives results in bathochromic shifts of absorption, fluorescence and phosphorescence compared to the reported aliphatic diketonate chelates. In fact, the absorption of the HPhN and HBAN difluoroboron chelates peaks at 450 nm and 459 nm, respectively, ($\epsilon_{450} = 10.2 \times 10^3 \text{ M}^{-1} \text{ cm}^{-1}$ and $\epsilon_{459} = 12.9 \times 10^3 \text{ M}^{-1} \text{ cm}^{-1}$). This enables

excitation with bright blue 450 nm and 470 nm LEDs and with conventional white light sources. Temperature affects the quantum yields of all three emissions. As expected, the phosphorescence QYs decrease at higher temperature and the delayed fluorescence becomes stronger (Fig. 2b). Since both phosphorescence and delayed fluorescence possess virtually identical decay times (Supplementary Fig. 1) and are quenched by oxygen to the same extent, their ratio can be used to eliminate temperature crosstalk. Importantly, prompt fluorescence is suitable for referencing purposes, as it is not affected by oxygen. However, the most outstanding property of these dyes is their extraordinary long phosphorescence decay time of 360 and 730 ms for BF₂(HPhN) and BF₂(HBAN), respectively (in polystyrene at 20°C), which, to the best of our knowledge, are the longest decay times recorded for visible light excitable dyes. This is likely due to the rigid aromatic backbone structure of the dyes. Despite those long decay times, the phosphorescence quantum yields are fairly high (Table 1, Supplementary Table 1).

Ultra sensitive oxygen sensing materials

Due to the exceptionally long lifetimes of these chelates, resulting sensing materials are expected to have sensitivities orders of magnitude above those based on conventional sensing chemistries. Indeed, sensors composed of difluoroboron chelates in polystyrene show very high sensitivities, even though polystyrene (PS) has only moderate oxygen permeability ($P \approx 8.8 \times 10^{-16} \text{ mol m}^{-1} \text{ s}^{-1} \text{ Pa}^{-1}$).²⁵ K_{sv} for BF₂(HPhN) and BF₂(HBAN) based sensors was $60 \times 10^{-3} \text{ ppmv}^{-1}$ and $120 \times 10^{-3} \text{ ppmv}^{-1}$ respectively, (Fig. 3a) which makes them suitable for monitoring sub-nanomolar DO concentrations. The limit of detection for the BF₂(HBAN)-based material, assuming a resolution of 0.5% I_0 , is in fact 45 ppbv (gas phase) or 60 pM (DO). Both sensing materials surpass the sensitivity of nearly all previously published sensors. Still, highly permeable matrices such as Hyflon®, Teflon® AF and poly(trimethylsilylpropyne) can potentially be used to create even more sensitive materials. Poly(trimethylsilylpropyne) has the highest known oxygen permeability ($P \approx 23000 \times 10^{-16} \text{ mol m}^{-1} \text{ s}^{-1} \text{ Pa}^{-1}$)²⁶ but was not considered due to poor chemical stability and possession of double bonds that are prone to oxidation and thus analyte consumption.^{27,28} Hyflon® and Teflon® AF are amorphous, glassy, perfluorinated copolymers that combine high free volume and unmatched chemical stability. In this work we used Hyflon® AD 60 ($P \approx 170 \times 10^{-16} \text{ mol m}^{-1} \text{ s}^{-1} \text{ Pa}^{-1}$).²⁹ and Teflon® AF 1600 ($P \approx 1200 \times 10^{-16} \text{ mol m}^{-1} \text{ s}^{-1} \text{ Pa}^{-1}$).³⁰ Unfortunately, most conventional dyes, as well as BF₂(HPhN) and BF₂(HBAN), show extremely poor solubility in these matrices and aggregate readily. We failed to obtain usable sensors based on the BF₂ chelates due to poor luminescence in perfluorinated polymers at any relevant concentration (0.01-1 % wt. of the dyes in respect to the polymer). Therefore, in order to render the indicators soluble in Hyflon® and Teflon® AF, HPhN and HBAN were perfluoroalkylated with perfluorooctyl iodide (Figure 1). The resulting ligands (HPhNPF and HBANPF) bear two C₈F₁₇ chains each, although in the case of HBANPF there is some impurity of tri-substituted ligand (Supplementary Fig. 2, 3). As indicated by NOESY and HMBC spectra (Supplementary Fig. 4, 5) a single isomer appears to be the predominant product for HPhNPF (Supplementary Fig. 6). The ¹H NMR and COSY spectra for HBANPF (Supplementary Fig. 7, 8) showed no significant substitution in the benzannulated ring. Complete separation of the tri-substituted derivate is very challenging due to the very high similarity; however both tri- and disubstituted derivatives are expected to

have very similar photophysical properties and solubility. It was found that perfluoroalkylated derivatives of the difluoroboron chelates have low chemical stability and dissociate in solution in presence of traces of water (Supplementary Fig. 9). Hence aluminium complexes ($\text{Al}(\text{HPhNPF})_3$ and $\text{Al}(\text{HBANPF})_3$, Figure 1) were prepared in an attempt to obtain more stable indicators. Indeed, dissociation was not observed for the aluminium chelates and they dissolve readily in fluorinated solvents (octafluorotoluene, perfluorodecalin) and also in Hyflon® and Teflon® AF. Due to the octahedral structure of the Al(III) complexes and unsymmetric substitution pattern of the ligands four stereoisomers are possible, which are inseparable because of their extreme similarity. The photophysical properties of the isomers are expected to be virtually identical. Similar to the BF_2 -chelates, the Al(III) complexes possess prompt fluorescence, delayed fluorescence and phosphorescence (Fig. 1). The phosphorescence decay times (250 ms for $\text{Al}(\text{HPhNPF})_3$ and 350 ms for $\text{Al}(\text{HBANPF})_3$ at 20°C in Teflon® AF 1600) are slightly shorter than those of the BF_2 -chelates and the Al(III) complexes possess higher molar absorption coefficients ($\epsilon_{465} = 23.2 \times 10^3 \text{ M}^{-1} \text{ cm}^{-1}$ and $\epsilon_{459} = 27.1 \times 10^3 \text{ M}^{-1} \text{ cm}^{-1}$ for $\text{Al}(\text{HPhNPF})_3$ and $\text{Al}(\text{HBANPF})_3$, respectively). The oxygen sensing materials based on these Al(III) complexes embedded in Hyflon® show extremely high sensitivities (Fig. 3b). In fact the K_{SV} values are as high as $590 \times 10^{-3} \text{ ppmv}^{-1}$ (for $\text{Al}(\text{HBANPF})_3$, Table 1) and the sensors resolve up to 10 ppbv or 12 pM DO. They are about one order of magnitude more sensitive than the state-of-the-art sensors based on fullerenes (Table 1).¹⁴ The sensors based on Teflon® AF 1600 show a 2-fold increase in sensitivity compared to the Hyflon®-based ones. $\text{Al}(\text{HBANPF})_3$ in Teflon® AF 1600 is the most sensitive sensor material presented, with a K_{SV} of $960 \times 10^{-3} \text{ ppmv}^{-1}$ and a detection limit of 5 ppbv or 7 pM. Potentially even more sensitive sensor materials based on Teflon® AF 2400 ($P \approx 3000 \times 10^{-16} \text{ mol m}^{-1} \text{ s}^{-1} \text{ Pa}^{-1}$)³⁰ showed signs of aggregation and were therefore not further investigated. Importantly, the Stern-Volmer plots for the phosphorescence decay time are similar to those obtained for the intensity measurements (Fig. 3b and supplementary Fig. 10) so both read-out schemes (ratiometric intensity or decay time) can be used. It should be mentioned, that sensitivities are so high that obtaining reliable calibrations becomes rather challenging. Even high purity nitrogen contains oxygen impurities in the low ppm range, hence all aluminium complex-based sensor materials were calibrated using a standard addition method described in the experimental section.

Temperature is known to affect the response of all optical sensors; thus the temperature dependence of the new sensors was investigated (Supplementary Fig. 11). In contrast to most oxygen sensors the Stern-Volmer constants K_{SV} decrease at higher temperature. This can be explained by a relatively strong effect of temperature on the phosphorescence decay time τ_0 (280, 250, 220 ms at 5, 20, 35 °C, respectively) and a negligible influence on the bimolecular quenching constant k_q (1.65, 1.65, 1.69 $\text{ppmv}^{-1} \text{ ms}^{-1}$ at 5, 20, 35 °C, respectively). This indicates that in contrast to most polymers the oxygen permeability of Hyflon® AD 60 appears to be barely affected by temperature.

Application example

To illustrate potential applications of these trace oxygen sensors, the kinetics of oxygen consumption during enzymatic oxidation of glucose was monitored as it approached anoxic

conditions (Fig. 4). Aqueous solutions of glucose oxidase (GOx), catalase and glucose were combined in a closed stirred vessel and the oxygen concentration was monitored with a set of sensors with overlapping ranges. Additionally to the Al(HPhNPF)₃/Hyflon® sensor two other oxygen sensors were used: a commercially available trace sensor from Pyroscience GmbH and a sensor based on Pd(II)-5,10,15,20-meso-tetrakis-(2,3,4,5,6-pentafluorophenyl)-porphyrin in Hyflon® which is comparable in sensitivity to previously published sensors.³¹ Figure 4 shows the high resolution of the new sensors in the ultra trace region, whereas the other sensors fail to resolve oxygen concentrations below 1 nM. The insert shows a mono exponential fit of the ultra trace region corresponding to purely diffusion-controlled depletion of oxygen.

Precise quantification of oxygen impurity in inert gases represents another potential application of the new sensors. The Al(HPhNPF)₃/Hyflon® sensor was used to quantify oxygen content in high purity gases obtained from Linde (Austria). For example, two samples of compressed nitrogen 5.0 (99.999%, < 10 ppmv O₂) contained 3.7 ppmv and 2.5 ppmv O₂ whereas compressed nitrogen 6.0 (99.9999%, < 1 ppmv O₂) contained 0.52 ppmv O₂ which is within the specifications of the gas manufacturer.

Discussion

We prepared new optical oxygen sensing materials with unmatched sensitivity. The most sensitive shows an approximate 20-fold increase in sensitivity compared to state-of-the-art materials. Such extraordinary high sensitivity results from the combination of extremely long phosphorescence decay times of the indicators and very high oxygen permeability of the matrix. Novel heavy metal-free chelates of rigid aromatic analogues of β-diketones represent unique indicators for oxygen sensors which feature absorption in the blue part of the electromagnetic spectrum, very long-decaying room-temperature phosphorescence, good molar absorption coefficients and adequate quantum yields. The unique dual emission of the chelates (delayed fluorescence and phosphorescence) can be used for intrinsic temperature compensation. These sensors enable completely new applications for monitoring of oxygen in previously inaccessible concentration regions, and are likely to become invaluable tools in various fields of science and technology.

Methods

Materials

Nitrogen (99.9999% purity), test gases (1000 ppm O₂, rest N₂ and 20 ppm O₂, rest N₂) were obtained from Linde Gas (Austria, www.linde.at), polystyrene (MW 250,000) and hydrogen peroxide (60%) were from Fisher Scientific. Perfluorooctyl iodide and aquaphobe™ CF were bought from ABCR (Germany, www.abcr.de). Teflon® AF 1600 was acquired from DuPont (USA, www.dupont.com). Hyflon® AD 60 was obtained from Solvay (USA, www.solvayplastics.com). Sodium sulfite was from Carl Roth (www.carlroth.com). Boron trifluoride diethyl etherate, aluminium oxide (activated, neutral Brockmann I), aluminium(III) chloride, 1,1,2-trichloro-1,2,2-trifluoroethane, glucose oxidase from *Aspergillus Niger*, catalase from bovine liver, anhydrous tetrahydrofurane and anhydrous dimethylsulfoxide were from Aldrich, iron(II) sulfate heptahydrate from Merck, sodium

hydroxide was from Lactan (Austria, www.lactan.at) and silicon E4 from Wacker (Germany, www.wacker.de). Acetone and ethanol were acquired from Brenntag (Germany, www.brenntag.de), and other solvents including the deuterated solvents were from VWR (Austria, <https://at.vwr.com>). 9-hydroxyphenalenone was obtained from Ramidus (Sweden, www.ramidus.se) and 6-hydroxybenz[de]anthracene-7-on was synthesized according to the literature procedure.²²

Synthesis of the BF₂chelate of 9-hydroxyphenalenone

294 mg (1.5 mmol) of 9-hydroxyphenalenone were dissolved in 50 ml of anhydrous tetrahydrofuran and 1.92 g (13.5 mmol) of boron trifluoride diethyl etherate were added. The solution was stirred for 1 h at 65 °C, the solvent was removed under vacuum and the product was purified on an aluminium oxide column using dichloromethane as an eluent. Yield: 300 mg (67 %) of orange crystals. ¹H NMR (300 MHz, DMSO-d₆, δ): 8.94 (d, J = 9.1 Hz, 2H), 8.70 (d, J = 7.7 Hz, 2H), 8.03 (t, J = 7.7 Hz, 1H), 7.62 (d, J = 9.1 Hz, 2H). EI-DI-TOF (m/z): found 244.0499, calcd 244.0510.

Synthesis of the BF₂chelate of 6-hydroxybenz[de]anthracene-7-on

369 mg (1.5 mmol) of 6-hydroxybenz[de]anthracene-7-on were dissolved in 60 ml of anhydrous tetrahydrofuran and 1.7 g (12 mmol) of boron trifluoride diethyl etherate were added. The solution was stirred at 65 °C for 2 h, 69 mg (0.5 mmol) of potassium carbonate were added and the stirring was continued for 2h. The solvent was removed under vacuum and the product was purified on an aluminium oxide column using dichloromethane as an eluent. Yield: 340 mg (77 %) of orange crystals. ¹H NMR (300 MHz, DMSO-d₆, δ): 9.26 (d, J = 7.7 Hz, 1H), 9.04 (d, J = 8.3 Hz, 1H), 8.91 (d, J = 9.2 Hz, 1H), 8.69 (d, J = 8.2 Hz, 1H), 8.50 (d, J = 7.6 Hz, 1H), 8.21 (t, J = 8.3 Hz, 1H), 7.97 (dt, J = 21.2, 7.6 Hz, 2H), 7.61 (d, J = 9.1 Hz, 1H). EI-DI-TOF (m/z): found 294.0671, calcd 294.0667.

Synthesis of C₈F₁₇substituted 9-hydroxyphenalenone

HPhN (1g, 5.1mmol) and FeSO₄ · 7 H₂O (2.5g, 9.0mmol) were dissolved in 120 mL DMSO and 40 mL 1,1,2-trichloro-1,2,2-trifluoroethane in a 200 mL Schlenk flask. The whole reaction was conducted under argon atmosphere. The solution was heated to 40 °C and perfluorooctyl iodide (3.4 mL, 7.03 g, 12.9 mmol) was added. 60 % H₂O₂ (1.4 mL, 1.67 g, 49 mmol) was added drop-wise over 5 min. The solution turned red and formed black foam. After 30 min 20 mL 1,1,2-trichloro-1,2,2-trifluoroethane were added and the foam dissolved. 1h after the start of the reaction a second portion perfluorooctyl iodide (3.4mL, 7.03g, 12.9mmol) was added and 60 % H₂O₂ (1.4 mL, 1.67 g, 49 mmol) was added drop-wise over 5 min. The reaction was continued for 1 h, then the reaction mixture was cooled to room temperature and the DMSO and 1,1,2-trichloro-1,2,2-trifluoroethane phases were separated. The 1,1,2-trichloro-1,2,2-trifluoroethane phase was washed 3 times with 36 % hydrochloric acid, once with water and was dried over Na₂SO₄. After removing the solvent 9.3 g reddish-brown oil were obtained. The product was purified on a silica-gel column with hexane and toluene as eluents. Yield: 700 mg (13 %). R_f 0.57 with toluene. ¹H NMR (300 MHz, CDCl₃, δ): 16.75 (s, 1H), 8.77 (s, 1H), 8.15-8.00 (m, 2H), 7.86 (d, J=7.9 Hz, 2H), 7.24 (d, J=9.3 Hz, 2H). DI-EI (m/z): 1031.98 found, 1031.98 calcd

Synthesis of C₈F₁₇substituted 6-hydroxybenz[de]anthracene-7-on

HBANPF was prepared using the same procedure as HPhNPF, but with a fivefold excess of perfluorooctyl iodide and the reaction mixture was stirred for 2 h at 40 °C and then overnight at room temperature. Yield 500 mg (23 %) starting from 0.5 g HBAN. Rf 0.69 with hexane/toluene 2/1. ¹H NMR (300MHz, CDCl₃, δ): 17.01 (s, 1H), 8.94 (s, 1H), 8.79 (d, J=8.2 Hz, 1H), 8.71 (d, J=7.9 Hz, 1H), 8.52 (d, J=8.3 Hz, 1H), 8.03 (d, J=8.2Hz, 1H), 7.89 (t, J=7.6Hz, 1H), 7.73 (t, J=7.5Hz, 1H). DI-EI (m/z): 1081.99 found, 1081.99 calcd

Synthesis of the aluminium complex of di-perfluorooctyl-9-hydroxyphenalenone

HPhNPF (100 mg, 0.097 mmol) was dissolved in 20 mL THF and 20 mL ethanol. NaOH (5.9 mg, 0.15 mmol) and AlCl₃ (3.9 mg, 29 μmol) were added and the reaction mixture was stirred for 2.5 h at 40 °C. Then the reaction was stopped the product was extracted with 1,1,2-trichloro-1,2,2-trifluoroethane and the organic phase was washed twice with water. The organic layer was dried over Na₂SO₄ and evaporated in vacuum. 5 mL THF were added to the raw product and the mixture was placed in the freezer for a few hours. The THF phase was removed and new THF was added. The product was washed 7 times following this procedure. Yield: 68.4 mg (74 %).: ¹H NMR (300 MHz, CDCl₃, δ): 8.87-8.55 (m, 3H), 8.15-7.84 (m, 6H), 7.84-7.54 (m, 3H), 7.42-7.04 (m, 3H); MALDI (m/z): [M+Na]⁺: 3142.93 found, 3142.90 calcd

Synthesis of the aluminium complex of di-perfluorooctyl-6-hydroxybenz[de]anthracene-7-on

Al(HBANPF)₃ was prepared and purified with the same procedure as Al(HPhNPF)₃. Yield 19.5mg (31%) starting from 80 mg HBANPF. ¹H NMR (300MHz, CDCl₃, δ): 9.2-8.2 (m, 9.9H), 8.06 (s, 3H), 8.0-7.2 (m, 7.2H); MALDI (m/z): [MH]⁺ : 3271.11 found, 3270.96 calcd, [MH(with one additional C₈F₁₇-Group)]⁺ : 3689.02 found, 3688.92 calcd

Preparation of the polystyrene-based sensing materials—The sensor “cocktails” contained the dyes (0.02% w/w in respect to the polymer), polystyrene (5% w/w in respect to the solvent) and chloroform. These were knife-coated on a glass slide using a 175 μm spacer. The resulting thickness for the dried layer is estimated to be 6 μm.

Preparation of the Hyflon® AD 60 based sensing materials—Prior to coating, the glass slides were rendered hydrophobic with aquaphobe™ CF. The dyes (0.05% w/w in respect to the polymer) and the polymer (6% w/w in respect to the solvent) were dissolved in octafluorotoluene. Knife-coating on the glass slides using a 175 μm spacer yielded a layer thickness of approximately 12 μm. After a second coating with a 275 μm spacer and evaporation of the solvent an about 31 μm-thick layer was obtained.

Preparation of the Teflon® AF 1600 based sensing materials—The sensors were prepared analogously to those based on Hyflon®, but a 5% w/w solution of the polymer in octafluorotoluene was used. The thickness of the sensing layer was estimated to be 24 μm.

Measurements—¹H NMR spectra were recorded on a 300 MHz instrument (Bruker). NOESY and HMBC spectra were acquired on an INOVA 500 MHz NMR-Spectrometer

(Varian). DMSO-d₆ was used for HPhN and HBAN and the respective BF₂ chelates and a mixture of 1,1,2-trichloro-1,2,2-trifluoroethane and CDCl₃ (1:1, v/v) was used for perfluorinated ligands and the respective chelates. Electron impact (EI, 70eV) and MALDI-TOF mass spectra were recorded on a Waters GCT Premier equipped with direct insertion (DI) and on a Micromass ToFSpec 2E, respectively. Absorption spectra were acquired on a Cary 50 UV-VIS spectrophotometer from Varian and the emission spectra on a Fluorolog 3 fluorescence spectrometer from Horiba Scientific equipped with a R2658 photomultiplier from Hamamatsu. The absolute luminescence quantum yields were determined using an integrating sphere from Horiba. The luminescence decay times for the sensing materials were measured with the Fluorolog 3 spectrometer in kinetic acquisition mode. Calibrations were obtained using a temperature-controlled flow through cell combined with a gas-mixing device from Voegtlin (Switzerland, www.red-y.com), which was used to mix nitrogen with 0.1 % O₂ test gas (for the boron chelates) and nitrogen with 20 ppm O₂ test gas (for the aluminium complexes). Calibrations for the aluminium complexes were further corrected for impurities in the nitrogen gas using a standard addition method, by measuring decay times under nitrogen and in oxygen-free sodium sulfite solution. The measured intensities under nitrogen were multiplied with the lifetime ratio (nitrogen/ oxygen-free) to obtain the actual value for I₀. All calibration points were corrected by the obtained intrinsic oxygen contamination. For additional information on photophysical properties of the dyes, see Supplementary Figures 12-16. For NMR and mass spec analysis of the compounds in this article, see Supplementary Figures 17-28.

Supplementary Material

Refer to Web version on PubMed Central for supplementary material.

Acknowledgements

The work was financially supported by the European Research Council (Project "Oxygen", N 267233). We thank Prof. R. Saf (Institute for Chemistry and Technology of Materials, Graz University of Technology) for acquiring mass spectra and Prof. H. Weber (Institute of Organic Chemistry) for acquiring and analysis of the NOESY and HMBC NMR spectra.

References

1. Tanno K. An Automatic Recording Analyzer for the Determination of Dissolved Oxygen in Boiler Feed Water. *Bull. Chem. Soc. Jpn.* 1964; 37:804–810.
2. Nakano T, Hoshi K, Baba S. Effect of background gas environment on oxygen incorporation in TiN films deposited using UHV reactive magnetron sputtering. *Vacuum.* 2008; 83:467–469.
3. Berger H. Contamination due to process gases. *Microelectron. Eng.* 1991; 10:259–267.
4. Longmuir IS. Respiration rate of bacteria as a function of oxygen concentration. *Biochem. J.* 1954; 57:81–87. [PubMed: 13159953]
5. Bergersen FJ, Turner GL. Bacterioids from Soybean Root Nodules: Respiration and NFormula-Fixation in Flow-Chamber Reactions with Oxyleghaemoglobin. *Proc. R. Soc. B.* 1990; 238:295–320.
6. Johnson MJ. Aerobic microbial growth at low oxygen concentrations. *J. Bacteriol.* 1967; 94:101–108. [PubMed: 6027987]
7. Stolper DA, Revsbech NP, Canfield DE. Aerobic growth at nanomolar oxygen concentrations. *Proc. Natl. Acad. Sci. U.S.A.* 2010; 107:18755–18760. [PubMed: 20974919]

8. Revsbech NP, et al. Determination of ultra-low oxygen concentrations in oxygen minimum zones by the STOX sensor. *Limnol Oceanogr Methods*. 2009; 7:371–381.
9. Kochmann S, Baleizão C, Berberan-Santos MN, Wolfbeis OS. Sensing and imaging of oxygen with parts per billion limits of detection and based on the quenching of the delayed fluorescence of (13)C70 fullerene in polymer hosts. *Anal. Chem.* 2013; 85:1300–1304. [PubMed: 23320578]
10. Crank, J.; Park, GS. *Diffusion in Polymers*. Marcel Dekker Inc.; 1996. p. 1-322.
11. Quaranta M, Borisov SM, Klimant I. Indicators for optical oxygen sensors. *Bioanal Rev.* 2012; 4:115–157. [PubMed: 23227132]
12. Wolfbeis OS. Materials for fluorescence-based optical chemical sensors. *J. Mater. Chem.* 2005; 15:2657–2669.
13. Amao Y. Probes and Polymers for Optical Sensing of Oxygen. *Microchim. Acta.* 2003; 143:1–12.
14. Wang X-D, Wolfbeis OS. Optical methods for sensing and imaging oxygen: materials, spectroscopies and applications. *Chem. Soc. Rev.* 2014; 43:3666–3761. [PubMed: 24638858]
15. Nagl S, Baleizão C, Borisov SM. Optical Sensing and Imaging of Trace Oxygen with Record Response. *Angew. Chem.* 2007; 46:2317–2319. [PubMed: 17323397]
16. Zhang G, Chen J, Payne SJ, Kooi SE. Multi-Emissive Difluoroboron Dibenzoylmethane Polylactide Exhibiting Intense Fluorescence and Oxygen-Sensitive Room-Temperature Phosphorescence. *J. Am. Chem. Soc.* 2007; 129:8942–8943. [PubMed: 17608480]
17. Zhang G, Palmer GM, Dewhirst MW, Fraser CL. A dual-emissive-materials design concept enables tumour hypoxia imaging. *Nat Mater.* 2009; 8:747–751.
18. Xu S, et al. Aromatic difluoroboron β -diketonate complexes: effects of π -conjugation and media on optical properties. *Inorg Chem.* 2013; 52:3597–3610.
19. Zhang X, Xie T, Cui M, Yang L, Sun X, Jiang J, Zhang G. General Design Strategy for Aromatic Ketone-Based Single-Component Dual-Emissive Materials *ACS Appl. Mater. Interfaces.* 2014; 6:2279–2284.
20. Borisov SM, Vasylevska AS, Krause C, Wolfbeis OS. Composite Luminescent Material for Dual Sensing of Oxygen and Temperature. *Adv. Funct. Mater.* 2006; 16:1536–1542.
21. Haddon RC, Rayford R, Hirani AM. 2-Methyl-and 5-methyl-9-hydroxyphenalenone. *J. Org. Chem.* 1981; 46:4587–4588.
22. Haddon RC. Benzannelated 9-hydroxyphenalenones. *Aust. J. Chem.* 1982; 35:1733.
23. Loudet A, Burgess K. BODIPY dyes and their derivatives: syntheses and spectroscopic properties. *Chem. Rev.* 2007; 107:4891–4932. [PubMed: 17924696]
24. Boens N, Leen V, Dehaen W. Fluorescent indicators based on BODIPY. *Chem. Soc. Rev.* 2012; 41:1130. [PubMed: 21796324]
25. Brandrup, J.; Immergut, EH.; Grulke, EA., editors. *Polymer Handbook*. Wiley; New York, USA: 1999.
26. Masuda T, Isobe E, Higashimura T, Takada K. Poly[1-(trimethylsilyl)-1-propyne]: a new high polymer synthesized with transition-metal catalysts and characterized by extremely high gas permeability. *J. Am. Chem. Soc.* 1983; 105:7473–7474.
27. Nagai K, Nakagawa T. Oxidation of poly(1-trimethylsilyl-1-propyne). *J. Appl. Polym. Sci.* 1994; 54:1651–1658.
28. Nagai K, Nakagawa T. Effects of aging on the gas permeability and solubility in poly (1-trimethylsilyl-1-propyne) membranes synthesized with various catalysts. *J. Membr. Sci.* 1995; 105:261–272.
29. Arcella V, Ghielmi A, Tommasi G. High Performance Perfluoropolymer Films and Membranes. *Ann. N. Y. Acad. Sci.* 2003; 984:226–244. [PubMed: 12783820]
30. Nemser, SM.; Roman, IC. Perfluorodioxole Membranes. US Patent 5051114 A filed 13 Jun. 1990, and issued 24 Sep. 1991.
31. Borisov SM, Lehner P, Klimant I. Novel optical trace oxygen sensors based on platinum(II) and palladium(II) complexes with 5,10,15,20-meso-tetrakis-(2,3,4,5,6-pentafluorophenyl)-porphyrin covalently immobilized on silica-gel particles. *Anal. Chim. Acta.* 2011; 690:108–115. [PubMed: 21414443]

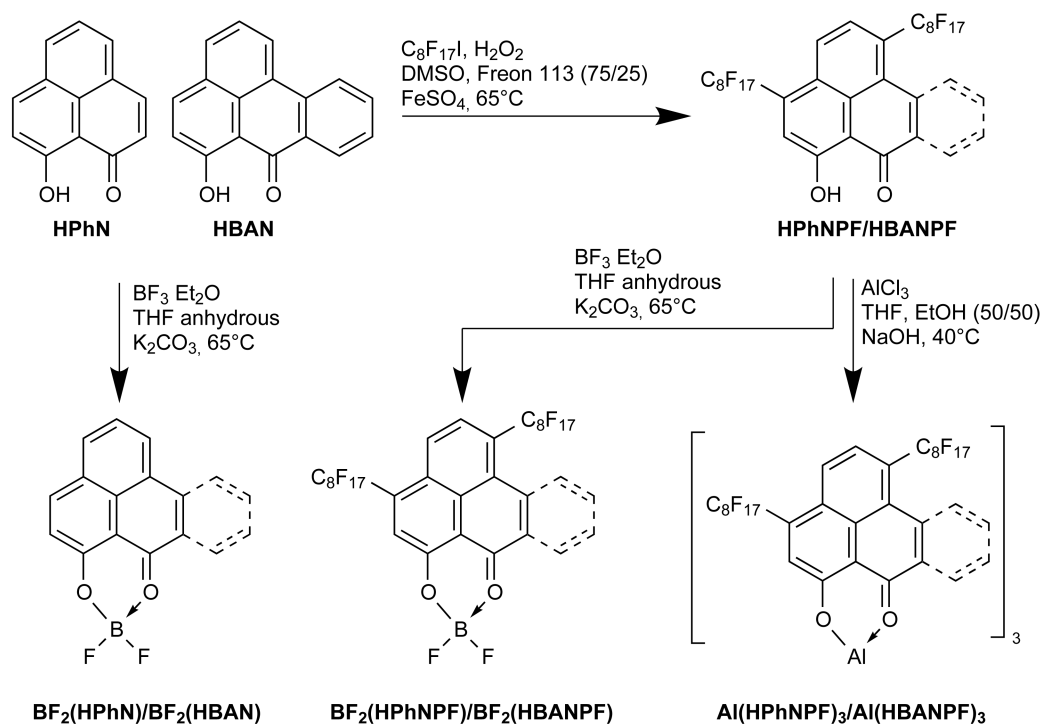


Figure 1. Synthesis of the borondifluoride chelates and aluminium complexes

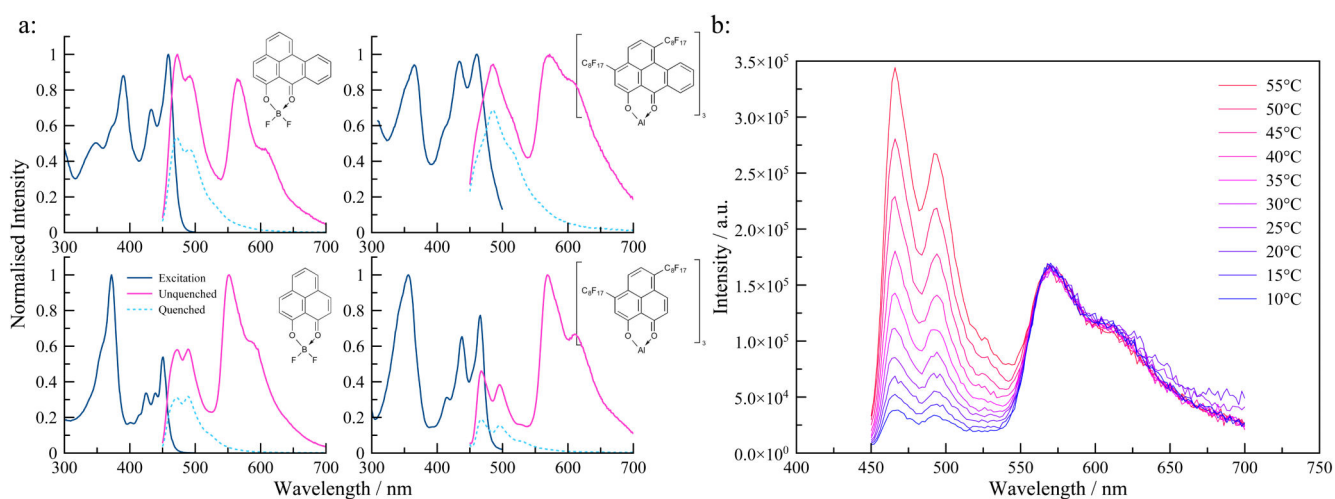


Figure 2. Spectral properties of the oxygen indicators

A: excitation and emission spectra of HBAN and HPhN difluoroboron chelates in polystyrene and aluminium complexes in Teflon® AF 1600; **b:** Temperature-dependent emission spectra of Al(HPhNPF)₃ in Hyflon® AD 60 under deoxygenated conditions acquired with a delay of 0.5 ms after excitation.

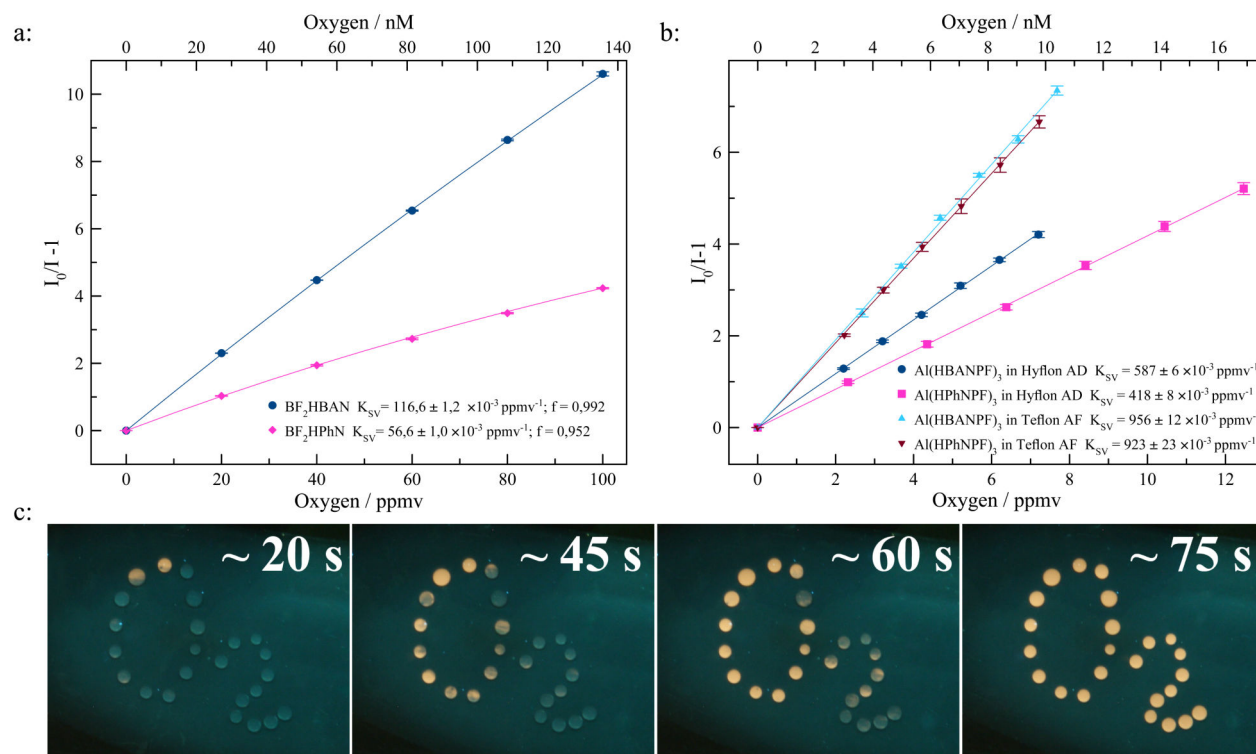


Figure 3. Oxygen sensitivity of the trace sensors at 20 °C

A: Stern-Volmer plots for BF_2HBAN and BF_2HPhN in polystyrene; **b:** Stern-Volmer plots for the aluminium complexes; **c:** photographic images of the $\text{Al}(\text{HPhNPF})_3/\text{Hyflon}^\circledR \text{AD } 60$ sensor under illumination with a 366 nm line of a UV lamp. Bluish prompt fluorescence remains constant, and the intense yellow phosphorescence slowly appears for the areas covered with anaerobic sodium sulfite solution (5% wt, containing traces of Co^{2+} as a catalyst).

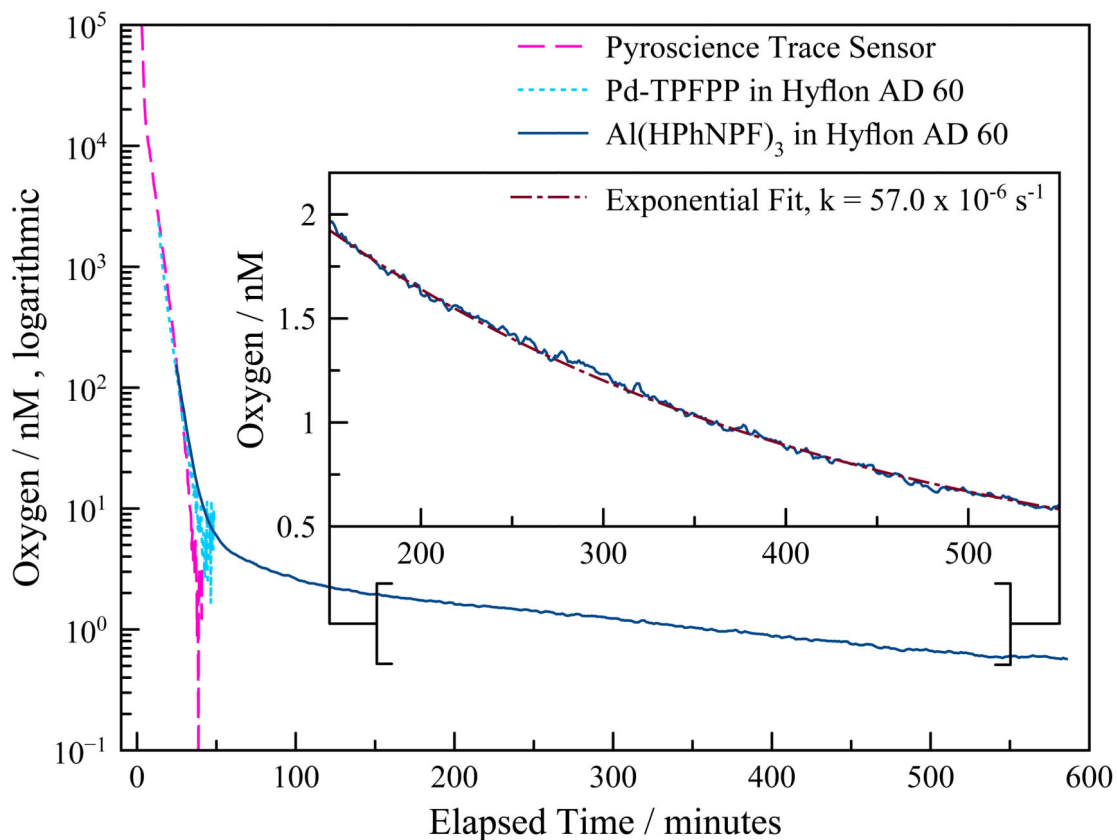


Figure 4. Real-time monitoring of oxygen levels during enzymatic oxygen consumption

Three trace sensors with overlapping ranges are used to monitor oxidation of glucose catalyzed by glucose oxidase. A running average of 3 data points was used for all sensors. Whereas the reference sensors fail to resolve below 2-10 nM, the new ultra trace sensor can reliably monitor oxygen even at much lower concentrations (insert).

Table 1
Photophysical and sensing properties of trace oxygen sensors at 20°C.

Sensor Material	Absorption max / nm [a]	Emission max. / nm	Φ / % [b]	τ_0 / ms	$K_{SV} / 10^{-3}$ ppmv ⁻¹	Reference
Pd-TPFP in Silica Gel	410	670	n.d.	0.978	7	[31]
C ₇₀ in Ethylcellulose	470	710	1 [c]	20-25	75	[15]
13C ₇₀ in Ethylcellulose [d]	470	710	n.d.	28	48	[9]
BF ₂ (HPhN) in polystyrene	450	552	4.6	360	60	[this work]
BF ₂ (HBAN) in polystyrene	459	565	9.1	730	120	[this work]
Al(HPhNPF) ₃ in Hyflon® AD 60	465	570	n.d.	270	420	[this work]
Al(HBANPF) ₃ in Hyflon® AD 60	459	565	n.d.	400	590	[this work]
Al(HPhNPF) ₃ in Teflon® AF 1600	465	570	5.4	250	920	[this work]
Al(HBANPF) ₃ in Teflon® AF 1600	459	575	3.2	350	960	[this work]

[a] the maximum for the longest wavelength absorption,

[b] Phosphorescence quantum yields,

[c] quantum yield of the delayed fluorescence,

[d] at 25°C